SUPPORTING INFORMATION

Protein Arginine Deiminase 2 Binds Calcium in an Ordered Fashion: Implications for Inhibitor Design

Daniel J. Slade[1, Δ], Pengfei Fang[2], Christina J. Dreyton[1, 7], Ying Zhang[3], Jakob Furhmann[1], Don Rempel[3], Benjamin, D. Bax[4], Scott A. Coonrod[5], Huw D. Lewis[6], Min Guo[2], Michael L. Gross[3], Paul R. Thompson[*1,7]

[1]Department of Chemistry, The Scripps Research Institute, Jupiter, FL 33458, USA.

[2]Department of Cancer Biology, The Scripps Research Institute, Jupiter, FL 33458, USA.

[3]Department of Chemistry, Washington University in St. Louis, MO 63130, USA.

[4]Molecular Discovery Research, GlaxoSmithKline, Medicines Research Centre, Gunnels Wood Road, Stevenage, Herts., SG1 2NY, UK.

[5]Department of Biomedical Sciences, Baker Institute for Animal Health, Cornell University, Ithaca, NY 14853, USA.

[6]EpiNova DPU, Immuno-Inflammation Therapy Area, GlaxoSmithKline, Medicines Research Centre, Gunnels Wood Road, Stevenage, Herts., SG1 2NY, UK.

[7]Department of Biochemistry and Molecular Pharmacology, University of Massachusetts Medical School, Worcester MA 01605.

[Δ]Currrent Address: Department of Biochemistry, Virginia Polytechnic Institute and State University, Blacksburg, VA 24061, USA.

FILES:

Supplementary Figure 1: PAD2 reaction and structural analysis
Supplementary Figure 2: The PAD2 Ca6 binding site is formed by a DxDxDG motif
Supplementary Figure 3: PAD2 calcium coordination
Supplementary Figure 4: Hydrogen deuterium exchange (HDX) mass spectrometry data confirms large conformational changes upon calcium binding

Figure S1

A.

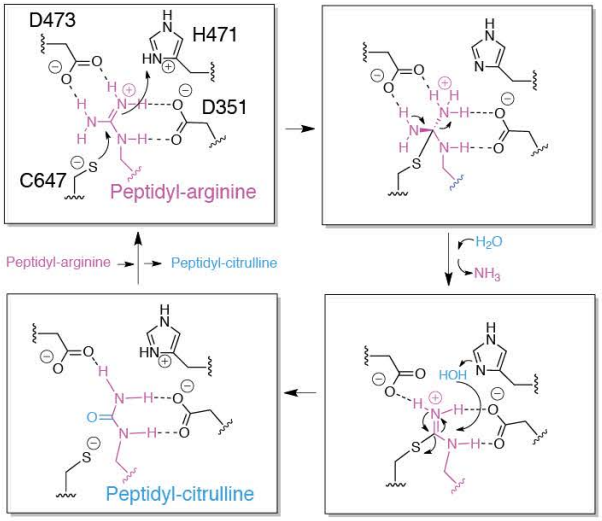

B.

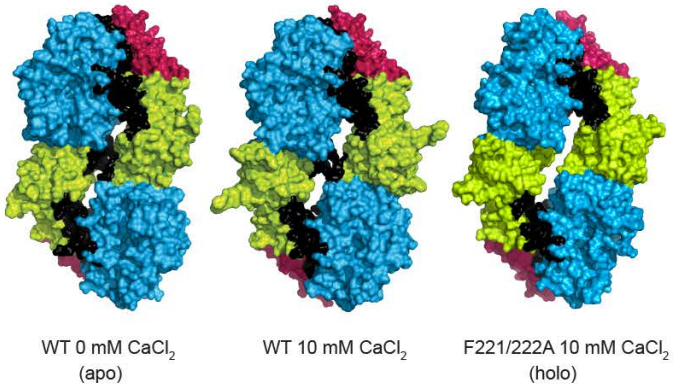

C.

	Apo	Holo
Number of residues		
Total	639 (100%)	653 (100%)
Surface exposed	587 (91.9%)	599 (91.7%)
Dimer interface	81 (12.7%)	78 (11.9%)
Solvent-accessible area (Å)		
Total	28,984.7 (100%)	29,145.3 (100%)
Dimer interface	2,551.8 (8.8%)	2,486.0 (8.5%)
Interfacing residues		
Salt bridges	18	16
Hydrogen bonds	30	30

D.

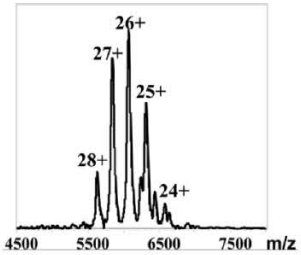

E.

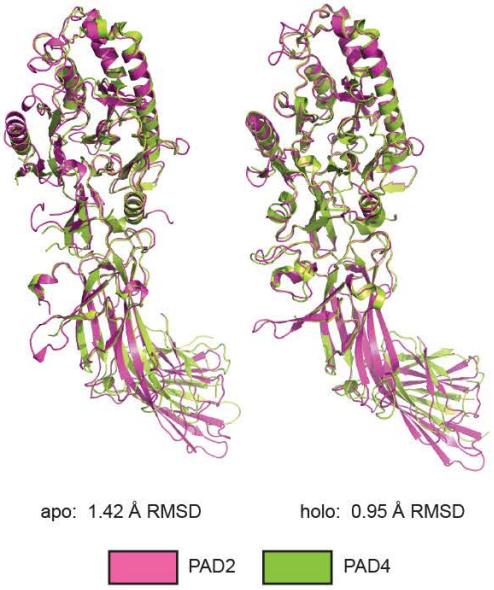

Figure S1. PAD2 reaction and structural analysis. (A) Proposed catalytic mechanism. (B) Surface representation of the apoPAD2 (*left*), PAD2•$Ca^{2+}_{(10\ mM)}$ (*middle*), and holoPAD2 (*right*) homodimers. (C) PAD2 statistics from the PDBePISA server shows that the confirmed homodimer is formed by a complex interface of two monomers arranged head to tail with interactions between IgG domain 1 and the C-terminal α/β propeller domain. The Complexation Significance Score (CSS) for the confirmed dimer was 0.191, and the CSS for the crystallographic dimer was 0.000. (D) Native mass spectrometry data of wild type PAD2 shows that it exists as a homodimer at 157.72 kDa, consistent with the theoretical homodimer mass of 157.14 kDa. (E) Structural alignment of apoPAD2 with apoPAD4 minus calcium (PDB: 1WD8) and holoPAD2 with holoPAD4 plus calcium (PDB: 1WD9) with the calculated root-mean-square deviation (RMSD) in angstroms.

Figure S2

A.

		DxDxDG
PAD1	(122-130)	DTGRTGKVK
PAD2	(123-131)	DADRDGVVE
PAD3	(122-130)	DLNCEGRQD
PAD4	(120-128)	DITRTGKVK
PAD6	(121-129)	DIYRNGQVE

B.

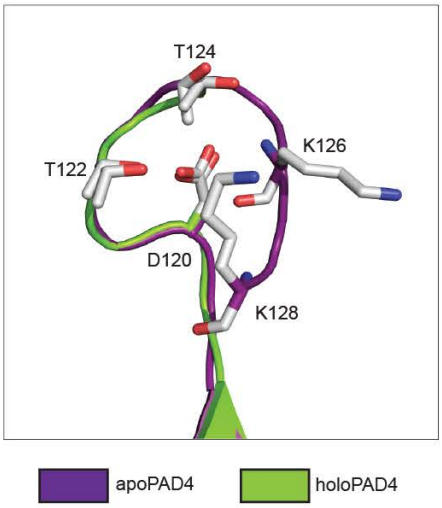

C.

		DxDxDG
hPAD2	(122-130)	DADRDGVVE
pPAD2	(123-131)	DADRDGVVE
bPAD2	(123-131)	DADRDGVVE
tPAD2	(122-130)	DADRDGVVE
xPAD2	(120-128)	DADRDGVVE
dPAD2	(121-129)	DADRDGVVE

D.

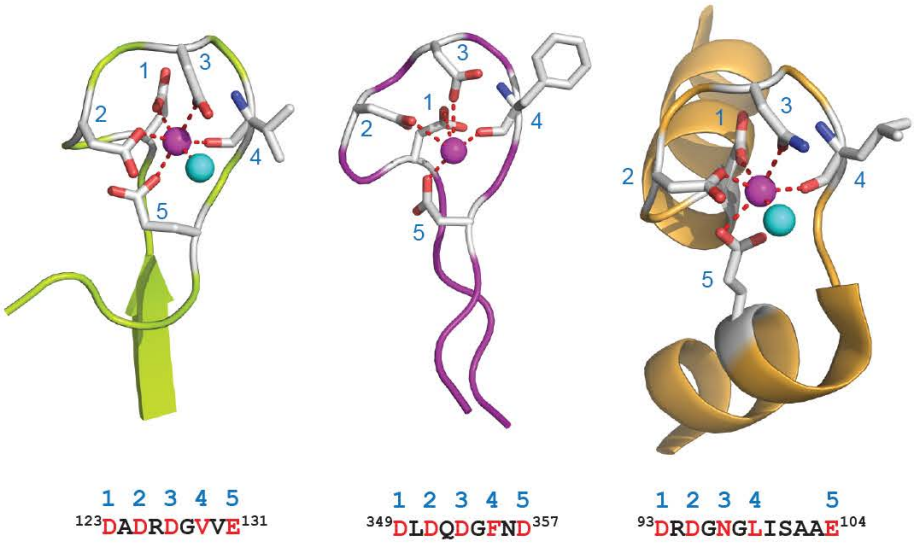

Figure S2. The PAD2 Ca6 binding site is formed by a DxDxDG motif. (A) Comparison of the PAD2 calcium 6 (Ca6) DxDxDG sequence within the human PADs. (B) Structural alignment of apoPAD4 (PDB: 1WD8) and holoPAD4 (PDB: 1WD9) shows that PAD4 does not bind a calcium in the same region as Ca6 in PAD2 because it lacks acidic residues. Despite the lack of calcium, this region adopts a similar fold to PAD2. (C) The DxDxDG motif is conserved in PAD2 from multiple species: hPAD2 = human (*Homo sapiens*), pPAD2 = chimpanzee (*Pan troglodytes*), bPAD2 = cattle (*Bos taurus*), tPAD2 = puffer fish (*Tetraodon nigroviridis*), xPAD2 = African clawed frog (*Xenopus laevis*), dPAD2 = zebrafish (*Danio rerio*). (D) The PAD2 Ca6 binding region is structurally related to folds found in human integrin (PDB: 1JV2) and calmodulin (PDB: 1EXR).

Figure S3

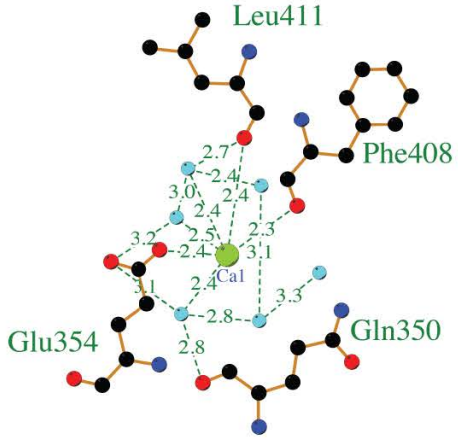

Calcium 1 - apoPAD2

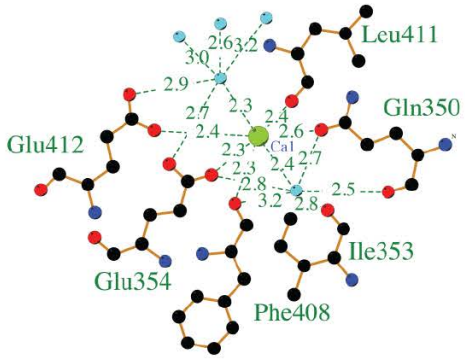

Calcium 1 - PAD2•Ca^{2+} (10 mM)

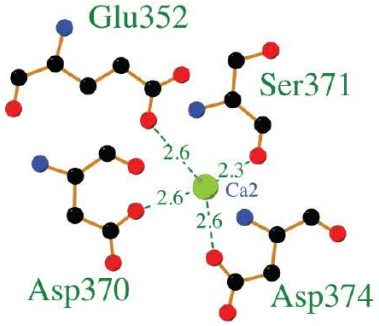

Calcium 2 - holoPAD2

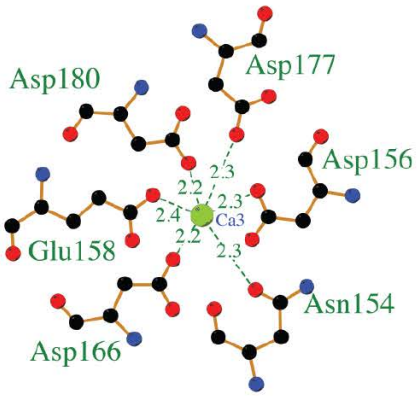

Calcium 3 - PAD2•Ca^{2+} (10 mM)

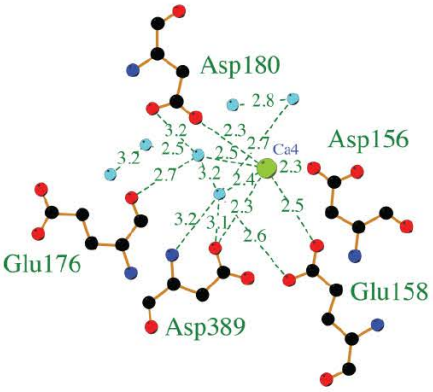

Calcium 4 - PAD2•Ca^{2+} (10 mM)

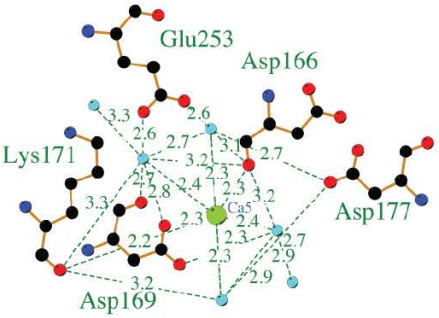

Calcium 5 - PAD2•Ca^{2+} (10 mM)

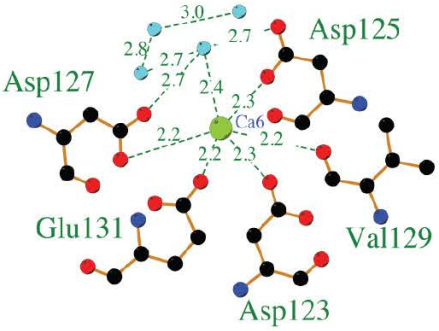

Calcium 6 - PAD2•Ca^{2+} (0 mM)

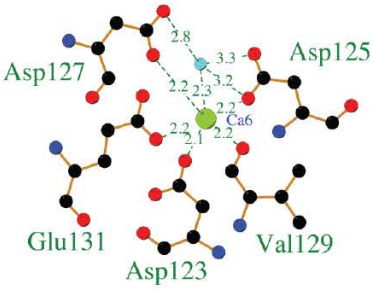

Calcium 6 - PAD2•Ca^{2+} (10 mM)

Figure S3. PAD2 calcium coordination. Coordination of the six calcium binding sites with labeled residues and bond distances. The ligand-protein interaction diagrams (Ligplots) show calcium-binding. Plots were created using LigPlot+.

Figure S4

A.

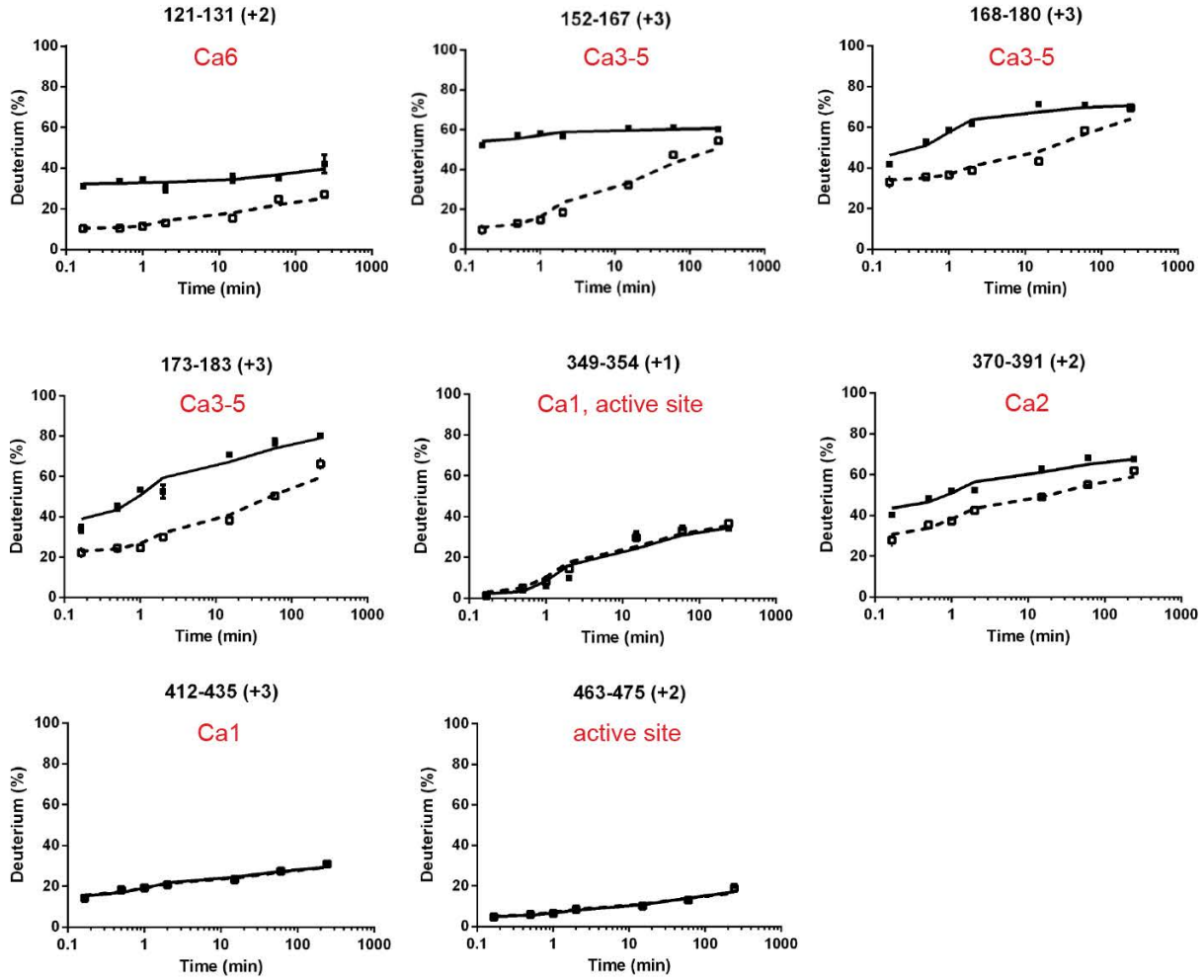

B.

Peptide (AA in PAD2)	Description of peptide region and HDX results
121-131	Encompasses Ca6 region and shows HDX + Ca^{2+}
152-167	Encompasses a portion of the Ca3-5 region and shows HDX + Ca^{2+}
168-180	Encompasses a portion of the Ca3-5 region and shows HDX + Ca^{2+}
173-183	Encompasses a portion of the Ca3-5 region and shows HDX + Ca^{2+}
349-354	Encompasses a portion of the Ca1 region and shows no HDX + Ca^{2+}
370-391	Encompasses a portion of the Ca2 region and shows HDX + Ca^{2+}
412-435	Encompasses a portion of the Ca1 region and shows no HDX + Ca^{2+}
463-475	Encompasses active site residues H471 and D473 and shows no HDX + Ca^{2+}

Figure S4. Hydrogen deuterium exchange (HDX) mass spectrometry data confirms large conformational changes upon calcium binding. (A) HDX kinetic plots for PAD2 reveal significant movements in the regions surrounding Ca2-6 in the presence and absence of calcium at 4 °C, and no movement for the Ca1 and active site regions. The apo state (no Ca^{2+}, solid line) exchanges more extensively than the holo state (2.5 mM Ca^{2+} dashed line), indicating higher flexibility in these regions. (B) Summary of HDX kinetics for each peptide and the corresponding regions in PAD2. The complete data set is included in Table S2.

Figure S5

A.

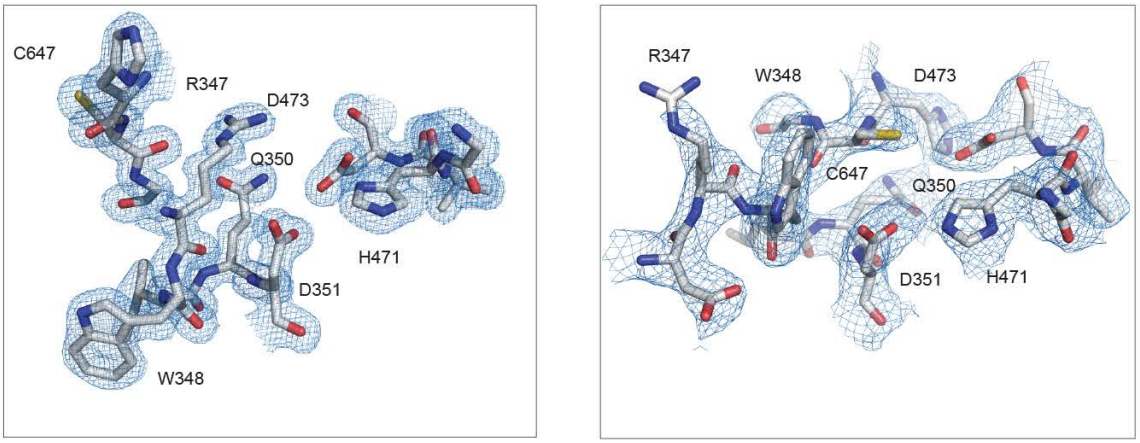

apo (0 mM $CaCl_2$) holo (10 mM $CaCl_2$)

B.

PAD1	(344-352)	NRNDRWIQD
PAD2	(343-351)	NRGDRWIQD
PAD3	(342-350)	NRNDRWIQD
PAD4	(342-350)	NMDDQWMQD
PAD6	(343-351)	NRLGRWLQD

Figure S5. Active-site rearrangement from apoPAD2 to holoPAD2. (A) Electron density from the apoPAD2 (left) and holoPAD2 (right) active sites in the 2Fo-Fc maps contoured at 1.0σ. Rearrangement of the active-site results in the relief of active-site shielding, which leads to proper positioning of the catalytic cysteine. (B) Sequence alignment of the five human PADs reveals that R347 is conserved, suggesting that active site shielding is a conserved regulatory mechanism.

Figure S6

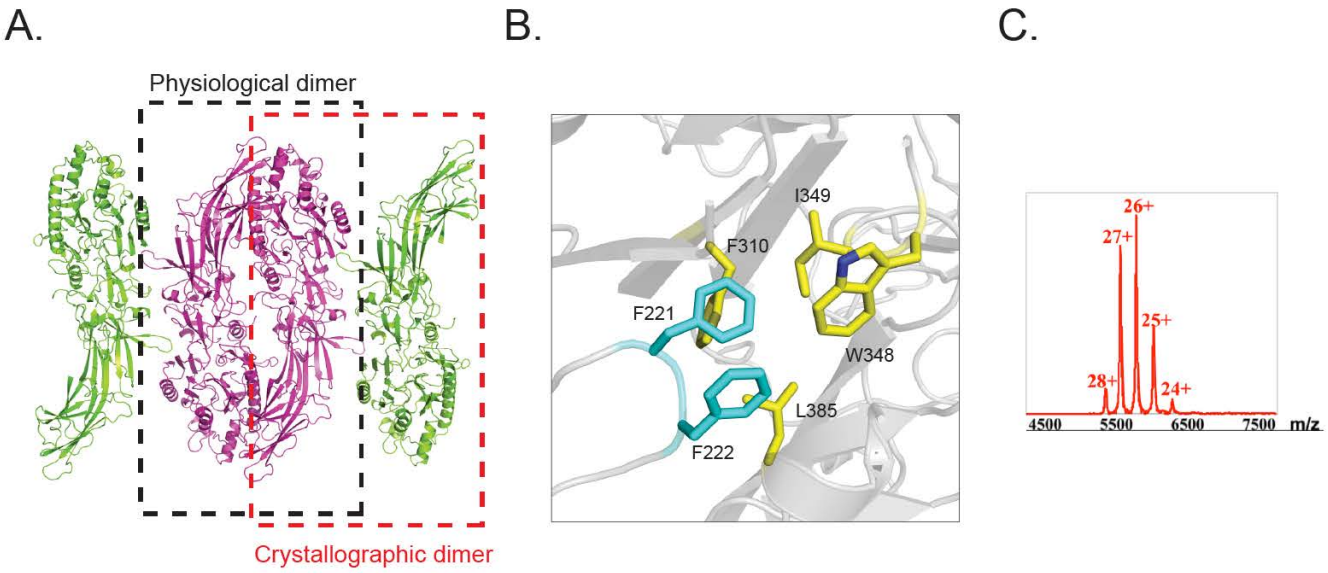

Figure S6. F221 and F222 form a crystal contact, but do not play a role in PAD2 dimerization. (A) View of PAD2 crystal packing, with the physiological PAD2 dimer in pink and outlined in black and the crystallographic dimer pink/green and outlined in red. (B) Zoomed view of F221 and F222 interacting with a hydrophobic pocket that is located on a neighboring subunit in the crystallographic lattice. (C) Native mass spectrometry data of PAD2 F221/222A shows that this mutant exists as a homodimer at 156.97 kDa, which is consistent with the theoretical masses of 156.83 kDa. Thus, these residues do not play a role in dimerization and the physiologically head-to-tail dimer is correct.

Figure S7

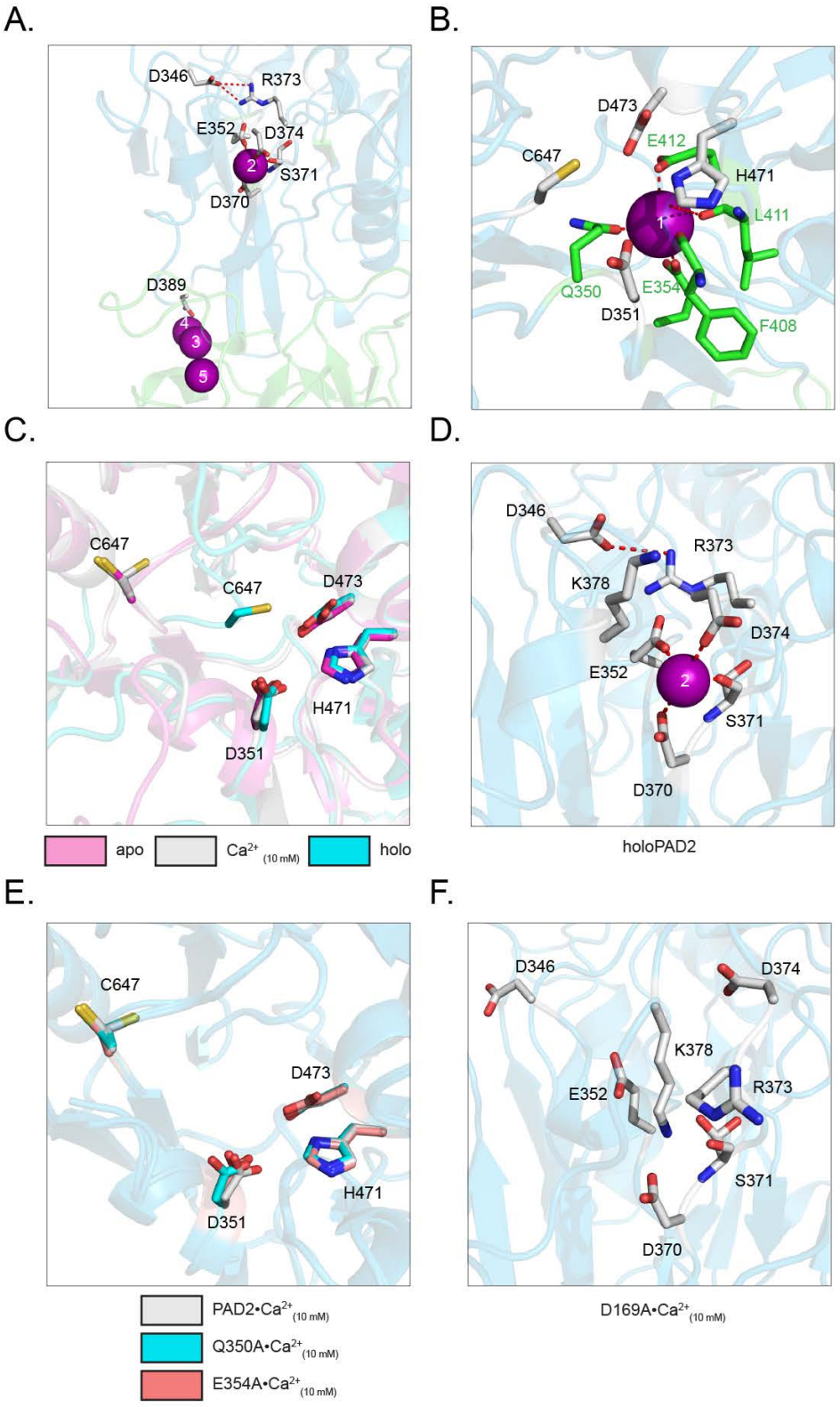

Figure S7: Analysis of PAD2 calcium-binding sites. (A) The calcium 2 (Ca2) binding site in the holoPAD2 structure. (B) The calcium 1 (Ca1) binding site from the holoPAD2 structure shows that it sits below the active site, and Q350 coordinates Ca1. Ca1 binding residues are in green and active site residues are in gray. (C) Structural alignment of apoPAD2, PAD•Ca2+$_{(10\ mM)}$, and holoPAD2 shows that the active site C647 is the only residue that moves, with D351, H471, and D473 remaining static. (D) Ca2 is occupied in holoPAD2 and forms a critical salt bridge between R373 and D346 that stabilizes the active site for catalysis. (E) Structural alignments of PAD2•$Ca^{2+}_{(10\ mM)}$, Q350A•$Ca^{2+}_{(10\ mM)}$, and E354A•$Ca^{2+}_{(10\ mM)}$ reveal that these mutations do not affect the position of the four active-site residues. RMSD for PAD•Ca2+$_{(10\ mM)}$ versus Q350A•Ca2+$_{(10\ mM)}$ and E354A•Ca2+$_{(10\ mM)}$ are 0.13 and 0.21 Å, respectively. (F) Comparision of the Ca2 binding region in D169A•$Ca^{2+}_{(10\ mM)}$ that is occupied by K378.

Figure S8

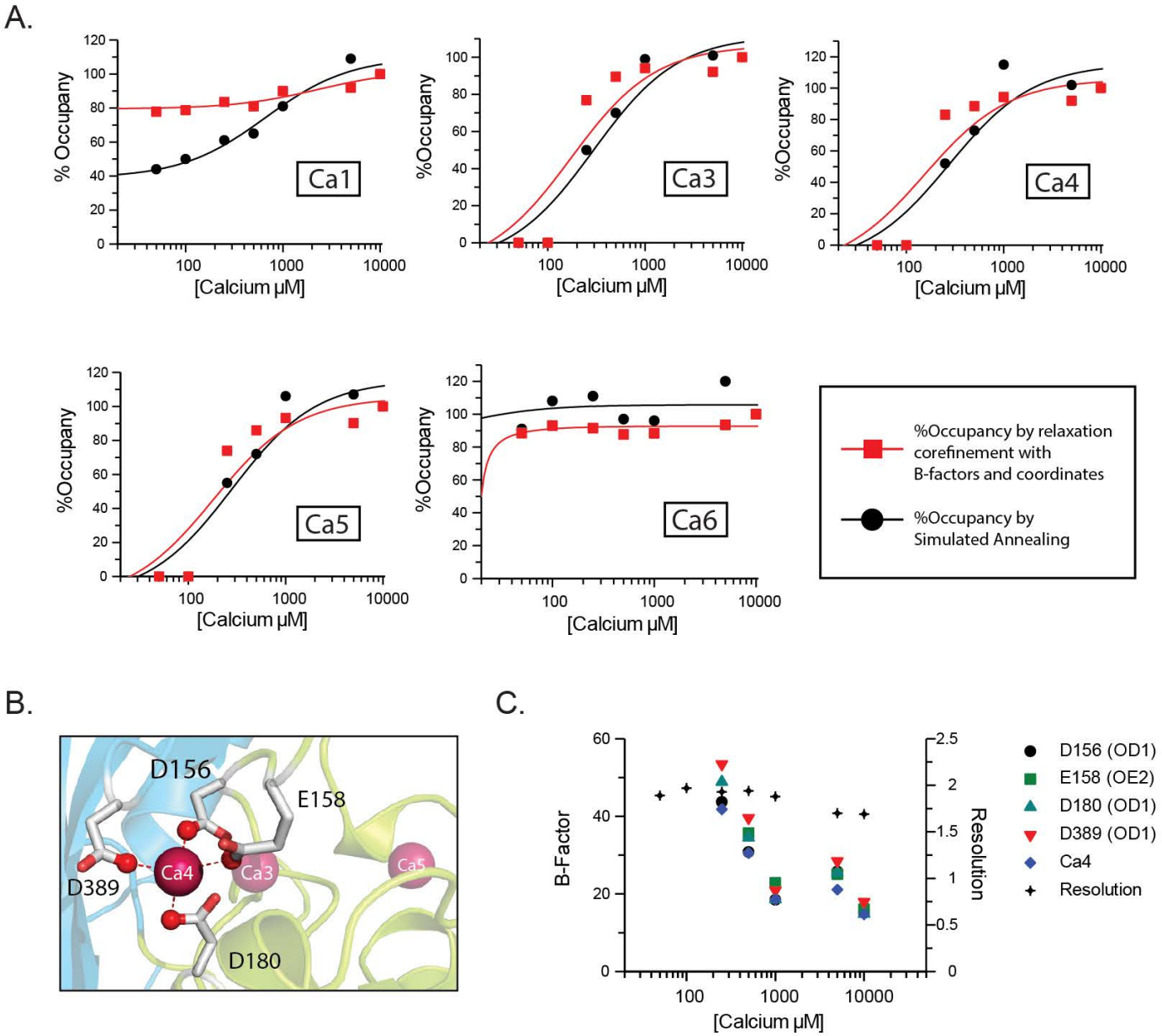

Figure S8. B-factors from calcium ions and calcium binding residues correlate with metal ion occupancy. (A) Comparison of calculated calcium occupancy for Ca1,3,4,5 by using B-factors (red) and e/Å^3 (black)(simulated annealing method) for each Ca^{2+} ion. (B) Four acidic residues coordinate Ca4, in which the metal ion binds in the PAD2 structures at concentrations of calcium $\geq$ 250 µM. (C) Soaking PAD2 crystals in increasing concentrations of $CaCl_2$ does not affect resolution (right axis), and therefore decreases in B-factors seen in the calcium ion and its coordinating residue are not a result of variation in resolution (left axis). B-factors of the oxygens that coordinate Ca4 from residues D156, E158, D180, and D389 are consistent with B-factors seen for Ca4 at 0, 50, 100, 250, 500, 1000, 5000, and 10000 µM soak concentrations. No data point for B-factor is present for E158 at 250 µM calcium as this residue does not coordinate Ca4 until $\geq$ 500 µM.

Supplementary Table 1 | PAD2 X-ray crystallography data collection and refinement statistics

	PAD2•$Ca^{2+}_{(0\ mM)}$	PAD2•$Ca^{2+}_{(10\ mM)}$	F221/222A•$Ca^{2+}_{(10\ mM)}$	PAD2•$Ca^{2+}_{(50\ \mu M)}$	PAD2•$Ca^{2+}_{(100\ \mu M)}$
PDB ID	4N20	4N2B	4N2C	4N22	4N24
Data collection[a]					
Space group	*C121*	*C121*	*C121*	*C121*	*C121*
Cell dimensions					
a, *b*, *c* (Å)	201.20, 51.86, 75.64	202.66, 51.54, 76.21	202.93, 52.18, 75.81	201.82, 51.64, 75.75	201.76, 51.58, 75.70
α, β, γ (ϒ)	90, 105.44, 90	90, 105.76, 90	90, 105.21, 90	90, 105.54, 90	90, 105.43, 90
Resolution (Å)	1.66	1.69	3.02	1.89	1.97
Wavelength (Å)	0.97875	0.97875	1.2836	1	1
R_{sym} or R_{merge}	0.066 (0.580)	0.078 (0.523)	0.083 (0.335)	0.080 (0.462)	0.111 (0.388)
$I/\sigma I$	23.5 (2.4)	17.6 (2.4)	17.0 (4.5)	15.6 (2.0)	10.8 (2.0)
Completeness (%)	100.0 (100.0)	99.4(93.9)	98.7 (89.3)	92.5 (64.9)	94.1(78.9)
Redundancy	5.2	4.1	4.1	4.1	3.8
Refinement					
Resolution (Å)	40.45-1.66	40.39-1.69	48.95-3.02	33.07-1.89	33.82-1.97
No. reflections	82,845	79,078	13,566	56,093	50,413
$R_{work/}$ R_{free}	17.1/20.3	16.8/20.1	24.5/27.2	16.9/20.7	17.4/21.6
No. atoms					
Protein	5197	5212	4997	5142	5039
Ligand/ion	30	37	6	31	42
Water	767	762	36	508	547
Average *B*-factors					
Protein	20	18.5	36.3	28.5	23.7
Ligand/ion	47.2	33.1	38.4	49.3	46.4
Water	31.2	29.7	33.1	35.8	31.7
r.m.s deviations					
Bond lengths (Å)	0.009	0.008	0.021	0.01	0.01
Bond angles (º)	1.298	1.347	0.959	1.2	1.29
Ramachandran					
Favored (%)	98.6	98.5	94.9	98.3	98.3
Disallowed (%)	0	0	0	0	0

Each data set was collected from a single crystal.

[a]Values in parentheses are for highest-resolution shell (10% of reflections).

Supplementary Table 1 | PAD2 X-ray crystallography data collection and refinement statistics

	PAD2•Ca^{2+} (250 μM)	PAD2•Ca^{2+} (500 μM)	PAD2•Ca^{2+} (1 mM)	PAD2•Ca^{2+} (5 mM)	D123N•Ca^{2+} (0 mM)
PDB ID	4N25	4N26	4N28	4N2A	4N2D
Data collection[a]					
Space group	*C121*	*C121*	*C121*	*C121*	*C121*
Cell dimensions					
a, *b*, *c* (Å)	202.27, 51.53, 75.99	202.27, 51.67, 76.09	202.68, 51.63, 76.27	203.42, 51.28, 76.37	202.19, 51.82, 75.89
α, β, γ (ϒ)	90, 105.56, 90	90, 105.54, 90	90, 105.57, 90	90, 105.69, 90	90, 105.65, 90
Resolution (Å)	1.93	1.94	1.88	1.7	2
Wavelength (Å)	1	1	1	0.9787	0.9787
R_{sym} or R_{merge}	0.084 (0.436)	0.087 (0.435)	0.104 (0.544)	0.064 (0.426)	0.075 (0.466)
$I/\sigma I$	16.5 (2.0)	14.7 (2.1)	13.8 (2.0)	11.6 (3.2)	16.7 (2.5)
Completeness (%)	96.6 (80.9)	93.8 (72.2)	95.1 (76.1)	99.8 (99.5)	99.9 (99.7)
Redundancy	4	4.1	4	4.2	3.7
Refinement					
Resolution (Å)	36.60-1.93	33.99-1.94	37.89—1.88	37.96-1.70	36.24-2.00
No. reflections	54,984	52,719	59,202	83,493	52,659
$R_{work/}$ R_{free}	17.9/22.1	16.9/22.2	17.2/21.6	16.9/19.6	17.7/22.3
No. atoms					
Protein	5022	5213	5243	5246	5031
Ligand/ion	33	33	44	45	26
Water	513	524	569	546	277
Average *B*-factors					
Protein	29.2	29.1	24.9	28.5	31.6
Ligand/ion	49	47	50.2	44.4	58.5
Water	35.5	34.7	33.2	37.2	32.6
r.m.s deviations					
Bond lengths (Å)	0.013	0.01	0.011	0.01	0.01
Bond angles (º)	1.22	1.24	1.23	1.21	1.31
Ramachandran					
Favored (%)	98.3	98.6	98.3	98.5	98.6
Disallowed (%)	0	0	0	0	0

Each data set was collected from a single crystal.

[a]Values in parentheses are for highest-resolution shell (10% of reflections).

Supplementary Table 1 | PAD2 X-ray crystallography data collection and refinement statistics

	D123N•$Ca^{2+}_{(10\ mM)}$	D169A•$Ca^{2+}_{(0\ mM)}$	D169A•$Ca^{2+}_{(10\ mM)}$	D177A•$Ca^{2+}_{(0\ mM)}$	D177A•$Ca^{2+}_{(10\ mM)}$
PDB ID	4N2E	4N2F	4N2G	4N2H	4N2I
Data collection[a]					
Space group	*C121*	*C121*	*C121*	*C121*	*C121*
Cell dimensions					
a, *b*, *c* (Å)	203.38, 51.91, 76.58	202.78, 51.02, 75.84	204.45, 50.94, 75.94	202.31, 52.30, 76.07	203.02, 51.47, 76.13
α, β, γ (ϒ)	90, 105.62, 90	90, 105.64, 90	90, 105.98, 90	90, 105.30, 90	90, 105.82, 90
Resolution (Å)	1.86	1.8	1.85	1.8	1.9
Wavelength (Å)	0.9787	0.9787	0.9787	0.9787	0.9787
R_{sym} or R_{merge}	0.106 (0.755)	0.076 (0.497)	0.068 (0.504)	0.083 (0.650)	0.075 (0.469)
$I/\sigma I$	15.1 (2.0)	9.9 (2.7)	11.6 (2.7)	18.6 (2.0)	10.5 (2.8)
Completeness (%)	99.7 (99.3)	100.0 (100.0)	100.0 (100.0)	99.1 (100.0)	100.0 (100.0)
Redundancy	4.2	4.2	4.2	4.1	4.2
Refinement					
Resolution (Å)	38.41-1.85	37.69-1.80	37.78-1.85	40.63-1.80	48.83-1.90
No. reflections	65,016	69,618	64,573	69,484	59,998
$R_{work/}$ R_{free}	16.8/20.7	17.1/20.1	17.8/21.6	17.2/21.0	17.1/20.9
No. atoms					
Protein	5203	5049	5164	5129	5233
Ligand/ion	37	38	54	26	48
Water	609	487	425	675	456
Average *B*-factors					
Protein	26.6	29.9	36.4	26.7	37.9
Ligand/ion	45.2	56.2	52.7	53.3	56.5
Water	35.2	36.6	40.8	35.5	40.9
r.m.s deviations					
Bond lengths (Å)	0.011	0.009	0.01	0.008	0.01
Bond angles (º)	1.31	1.21	1.25	1.26	1.23
Ramachandran					
Favored (%)	98.3	98.2	97.9	98.6	97.7
Disallowed (%)	0	0	0	0	0

Each data set was collected from a single crystal.

[a]Values in parentheses are for highest-resolution shell (10% of reflections).

Supplementary Table 1 | PAD2 X-ray crystallography data collection and refinement statistics

	Q350A•$Ca^{2+}_{(0\ mM)}$	Q350A•$Ca^{2+}_{(10\ mM)}$	E354A•$Ca^{2+}_{(0\ mM)}$	E354A•$Ca^{2+}_{(10\ mM)}$
PDB ID	4N2K	4N2L	4N2M	4N2N
Data collection[a]				
Space group	*C121*	*C121*	*C121*	*C121*
Cell dimensions				
a, *b*, *c* (Å)	202.24, 51.94, 75.96	203.38, 51.10, 76.18	202.26, 51.63, 76.19	203.20, 51.63, 76.54
α, β, γ (ϒ)	90, 105.31, 90	90, 105.60, 90	90, 105.59, 90	90, 106.04, 90
Resolution (Å)	1.57	2.1	1.6	1.8
Wavelength (Å)	0.9787	0.9787	0.9787	0.9787
R_{sym} or R_{merge}	0.071 (0.489)	0.097 (0.427)	0.066 (0.660)	0.094 (0.536)
$I/\sigma I$	26.8 (2.0)	9.1 (3.1)	26.8 (2.0)	8.1 (2.3)
Completeness (%)	96.7 (93.5)	99.9 (99.7)	99.5 (98.6)	99.5 (99.0)
Redundancy	4.2	4.1	4.2	4.2
Refinement				
Resolution (Å)	40.58-1.57	40.24-2.10	42.66-1.60	38.06-1.80
No. reflections	103,006	44,320	99,810	70,612
$R_{work/}$ R_{free}	17.7/20.8	16.5/21.5	17.7/20.3	16.9/20.1
No. atoms				
Protein	5149	5208	5211	5253
Ligand/ion	32	65	37	36
Water	711	421	653	653
Average *B*-factors				
Protein	24.9	32.2	26.6	28.2
Ligand/ion	49.3	53.6	57	43.6
Water	35.3	36.3	35.7	37.2
r.m.s deviations				
Bond lengths (Å)	0.007	0.011	0.007	0.01
Bond angles (º)	1.24	1.22	1.26	1.23
Ramachandran				
Favored (%)	98.6	98	98.4	98.5
Disallowed (%)	0	0	0	0

Each data set was collected from a single crystal.

[a]Values in parentheses are for highest-resolution shell (10% of reflections).

Supplementary Table 2 | Description of PAD2 peptic peptides and HDX Data.

Peptide (AA in PAD2)	Description of peptide and HDX results
121-131	Encompasses Ca6 region and shows differences in HDX $\pm$ Ca^{2+}
121-151	Encompasses Ca6 region and shows differences in HDX $\pm$ Ca^{2+}
121-151	Encompasses Ca6 region and shows differences in HDX $\pm$ Ca^{2+}
152-155	Precedes the Ca3-5 region and shows differences in HDX $\pm$ Ca^{2+}
152-167	Encompasses a portion of the Ca3-5 region and shows differences in HDX $\pm$ Ca^{2+}
156-176	Encompasses a portion of the Ca3-5 region and shows differences in HDX $\pm$ Ca^{2+}

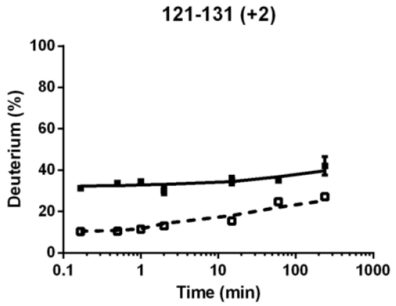

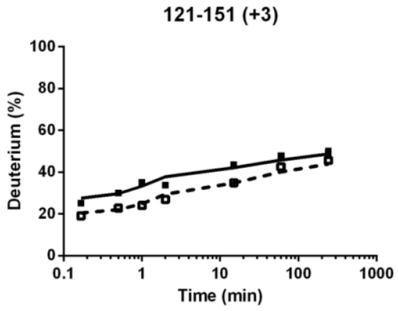

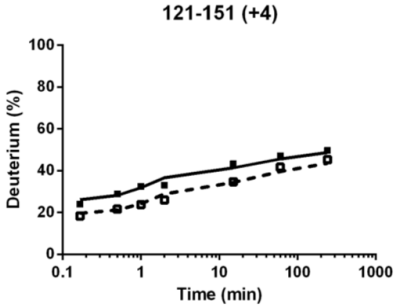

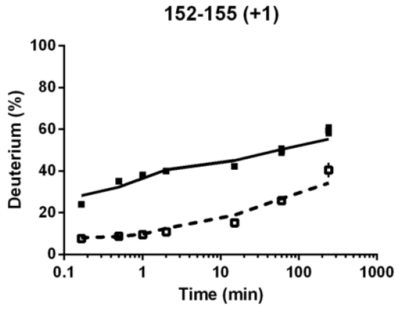

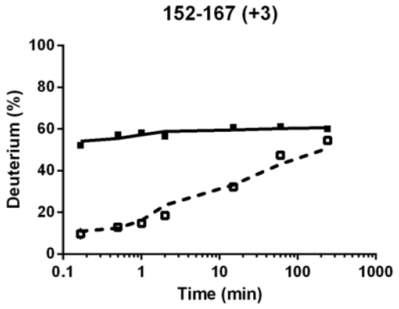

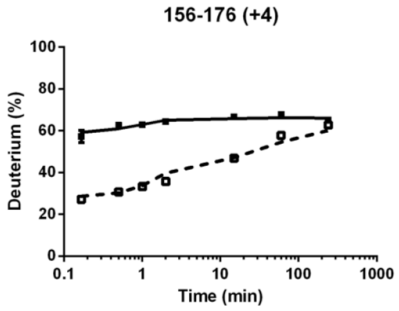

Supplementary Table 2 | Description of PAD2 peptic peptides and HDX Data.

Peptide (AA in PAD2)	Description of peptide and HDX results
156-180	Encompasses a portion of the Ca3-5 region and shows differences in HDX ± Ca^{2+} 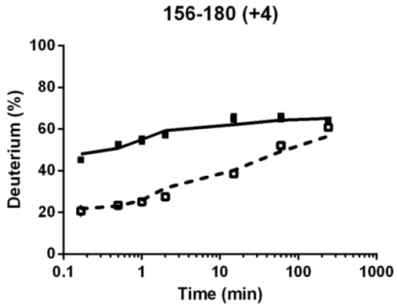
156-180	Encompasses a portion of the Ca3-5 region and shows differences in HDX ± Ca^{2+} 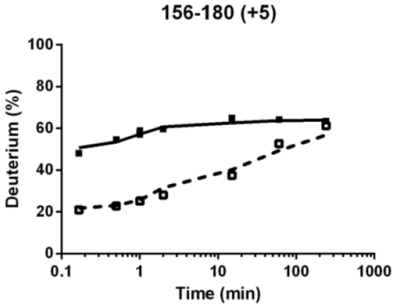
168-172	Encompasses a portion of the Ca3-5 region and shows differences in HDX ± Ca^{2+} 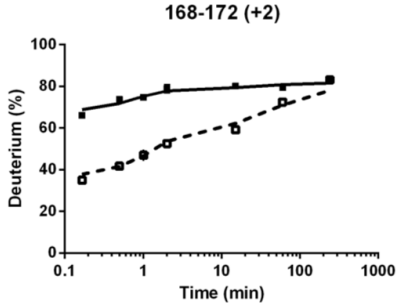
168-176	Encompasses a portion of the Ca3-5 region and shows differences in HDX ± Ca^{2+} 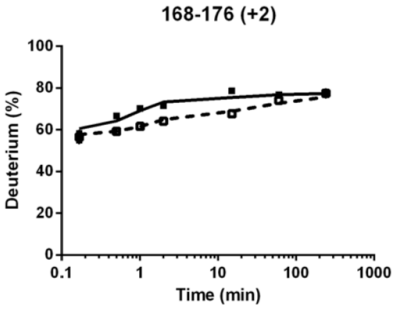
168-176	Encompasses a portion of the Ca3-5 region and shows differences in HDX ± Ca^{2+} 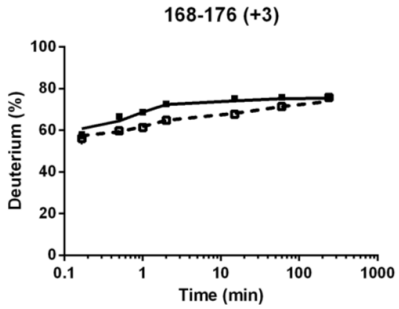
168-180	Encompasses a portion of the Ca3-5 region and shows differences in HDX ± Ca^{2+} 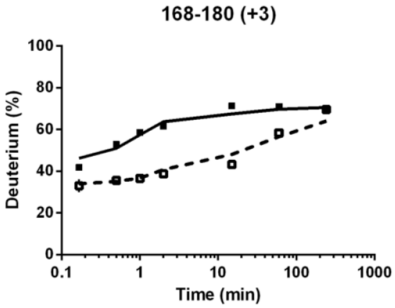

Supplementary Table 2 | Description of PAD2 peptic peptides and HDX Data.

Peptide (AA in PAD2)	Description of peptide and HDX results
168-180	Encompasses a portion of the Ca3-5 region and shows differences in HDX ± Ca^{2+} 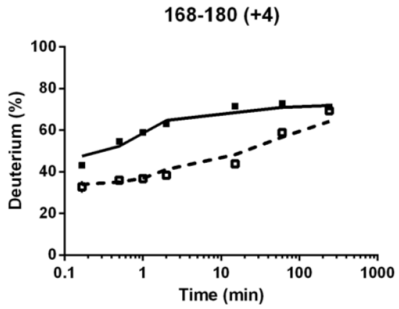
173-180	Encompasses a portion of the Ca3-5 region and shows differences in HDX ± Ca^{2+} 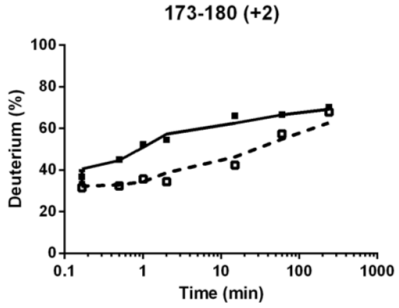
173-180	Encompasses a portion of the Ca3-5 region and shows differences in HDX ± Ca^{2+} 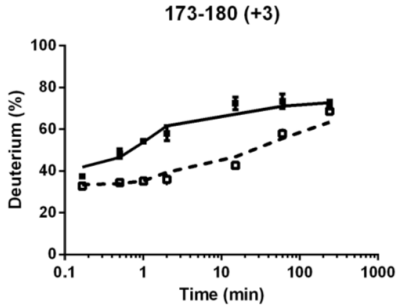
173-183	Encompasses a portion of the Ca3-5 region and shows differences in HDX ± Ca^{2+} 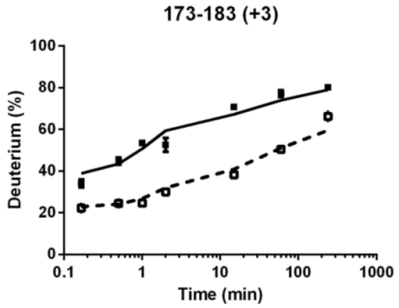
349-354	Encompasses active site residues D351 and shows no differences in HDX ± Ca^{2+} 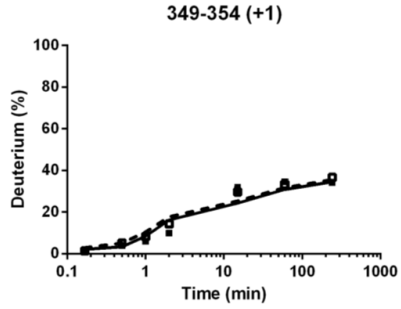
370-377	Encompasses a portion of the Ca2 region and shows differences in HDX ± Ca^{2+} 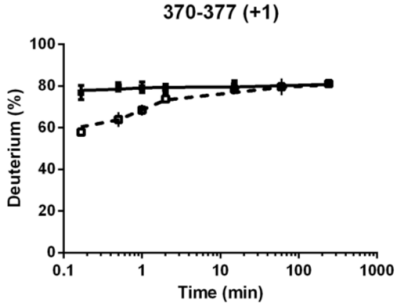

Supplementary Table 2 | Description of PAD2 peptic peptides and HDX Data.

Peptide (AA in PAD2)	Description of peptide and HDX results
370-377	Encompasses a portion of the Ca2 region and shows differences in HDX ± Ca^{2+} 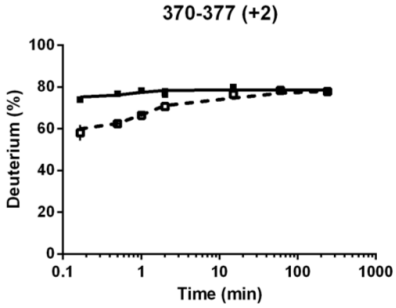
370-379	Encompasses a portion of the Ca2 region and shows differences in HDX ± Ca^{2+} 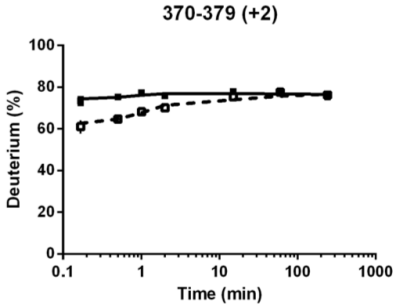
370-379	Encompasses a portion of the Ca2 region and shows differences in HDX ± Ca^{2+} 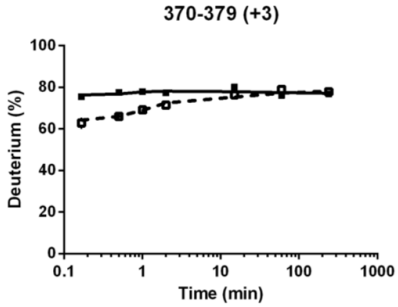
370-384	Encompasses a portion of the Ca2 region and shows differences in HDX ± Ca^{2+} 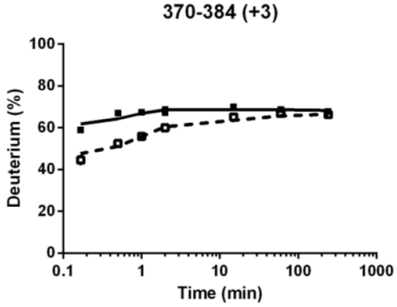
370-391	Encompasses a portion of the Ca2 region and shows differences in HDX ± Ca^{2+} 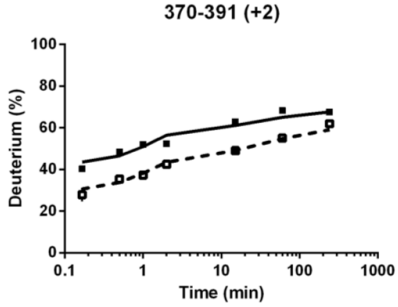
370-391	Encompasses a portion of the Ca2 region and shows differences in HDX ± Ca^{2+} 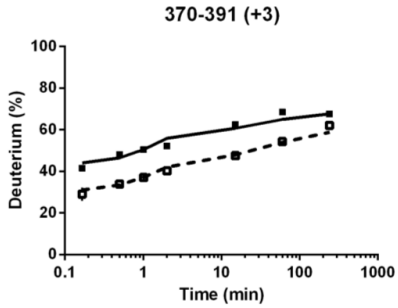

Supplementary Table 2 | Description of PAD2 peptic peptides and HDX Data.

Peptide (AA in PAD2)	Description of peptide and HDX results
370-391	Encompasses a portion of the Ca2 region and shows differences in HDX ± Ca^{2+} 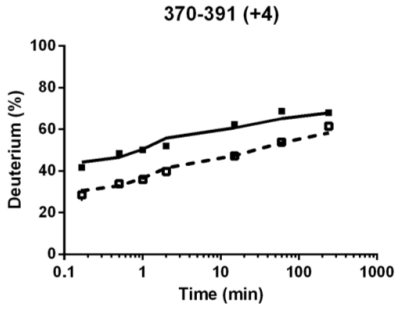
370-392	Encompasses a portion of the Ca2 region and shows differences in HDX ± Ca^{2+} 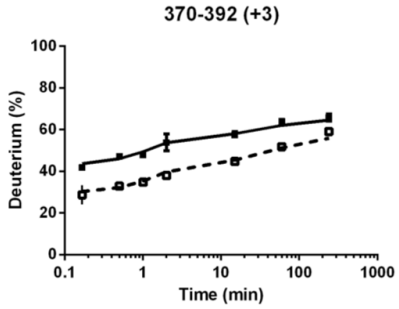
378-391	Encompasses a portion of the Ca2 region and shows differences in HDX ± Ca^{2+} 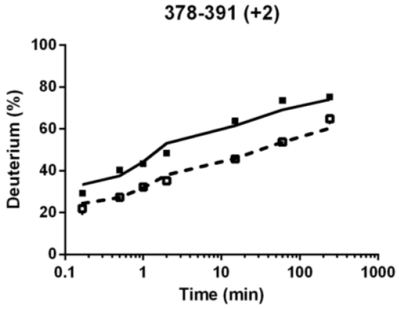
378-391	Encompasses a portion of the Ca2 region and shows differences in HDX ± Ca^{2+} 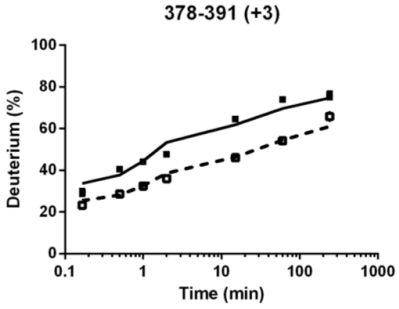
380-391	Encompasses a portion of the Ca2 region and shows differences in HDX ± Ca^{2+} 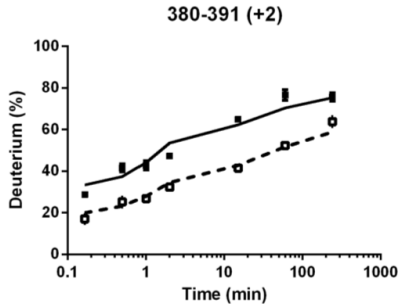
412-430	Encompasses a portion of the Ca1 region and shows no differences in HDX ± Ca^{2+} 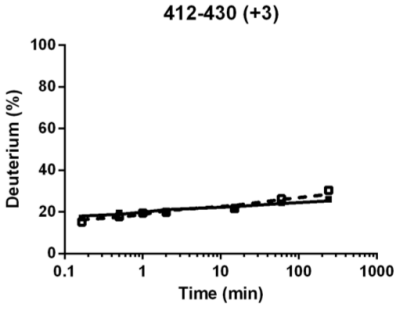

Supplementary Table 2 | Description of PAD2 peptic peptides and HDX Data.

Peptide (AA in PAD2)	Description of peptide and HDX results
412-432	Encompasses a portion of the Ca1 region and shows no differences in HDX ± Ca^{2+} 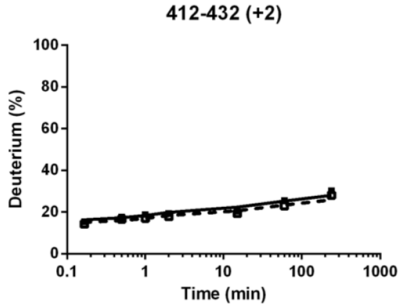
412-432	Encompasses a portion of the Ca1 region and shows no differences in HDX ± Ca^{2+} 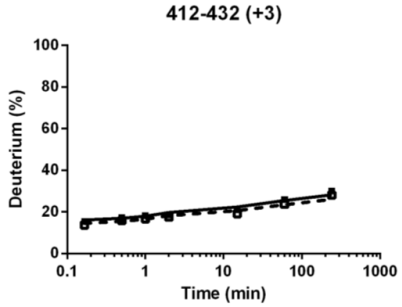
412-434	Encompasses a portion of the Ca1 region and shows no differences in HDX ± Ca^{2+} 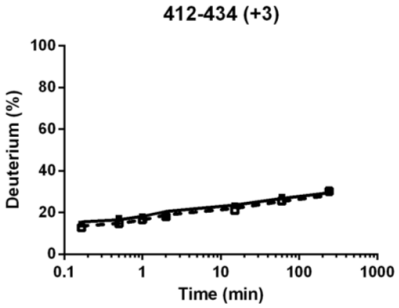
412-435	Encompasses a portion of the Ca1 region and shows no differences in HDX ± Ca^{2+} 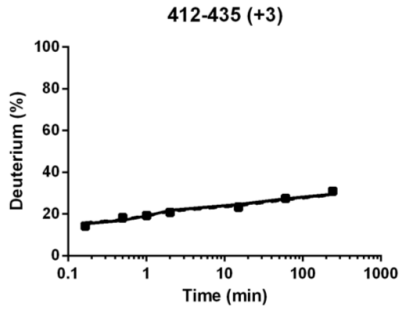
463-475	Encompasses active site residues H471 and D473 and shows no differences in HDX ± Ca^{2+}